

# Macroporous silicon with a complete two-dimensional photonic band gap centered at 5 $\mu\text{m}$

U. Grüning<sup>a)</sup> and V. Lehmann  
*Siemens AG, ZFE T ME 1, Otto-Hahn-Ring 6, 81730 München, Germany*

S. Ottow  
*Institute of Materials Science, University of Kiel, Kaiserstrasse 2, 24143 Kiel, Germany*

K. Busch  
*Institute for Theory of Condensed Matter, University of Karlsruhe, 76128 Karlsruhe, Germany*

(Received 25 September 1995; accepted for publication 29 November 1995)

We have fabricated a two-dimensional photonic band structure based on macroporous silicon with a gap common to both polarizations and centered at 5  $\mu\text{m}$ . A triangular lattice of circular air rods with a lattice constant of 2.3  $\mu\text{m}$  was etched 75  $\mu\text{m}$  deep in an *n*-type silicon substrate by electrochemical pore formation in hydrofluoric acid. The porous layer was then micromechanically structured in such a way that 200  $\mu\text{m}$  thick free-standing bars of porous material were left over on the silicon substrate. These bars were then used for measuring the transmission of the photonic lattice. The results showed an excellent agreement with the theoretically calculated structure.  
© 1996 American Institute of Physics. [S0003-6951(96)04006-6]

The existence of a photonic band gap in dielectric or metallic structures that are periodic on a wavelength scale has recently received much attention.<sup>1-5</sup> The propagation of radiation in such structures can be described similar to the case of electrons propagating in a crystal. A band gap can open up, i.e., a frequency range exists where electrons or photons are not allowed to propagate in any direction. The changed mode density in the gap region can lead to interesting phenomena such as a changed spontaneous emission behavior of atoms.<sup>1</sup> Improved and new optical components can be expected from such an artificially tailored optical material.<sup>6</sup>

The mechanical fabrication of photonic band structures in the centi- and millimeter wavelength range in two,<sup>7-9</sup> and three<sup>10-13</sup> dimensions allowed the verification of theoretical calculations.<sup>14-18</sup> Scaling down to optical and infrared frequencies, however, leads to the limits of today's technology due to the uniformity and regularity demanded of the photonic lattice on less than a wavelength scale.<sup>19-21</sup>

By electrochemical etching in hydrofluoric acid, macroporous silicon can be formed in a regular pattern of uniform pores with a diameter in the micrometer range and a depth of several hundreds of micrometers.<sup>22</sup> This technique has been proven to meet the requirements for fabricating an infrared photonic band gap material.<sup>23</sup>

In this letter, we report the first fabrication of free-standing bars of macroporous silicon with a depth of 75  $\mu\text{m}$ , a width of 200  $\mu\text{m}$ , and feature sizes as small as 170 nm. The transmission spectra show a complete two-dimensional photonic band gap centered at 4.9  $\mu\text{m}$  and are in excellent agreement with theoretical calculations.

First the sample preparation will be briefly explained. The details of the electrochemical pore formation process are published in detail elsewhere.<sup>22</sup> Only a short description will be given here. Macropores with micrometer pore radii can be

formed in the  $\langle 100 \rangle$  direction in moderately doped *n*-type silicon if it is anodized in a hydrofluoric acid solution while the backside of the wafer is illuminated. If this process is applied to a polished silicon substrate, the pores will grow in a random pattern. However, for example, if etch pits generated by standard lithography and alkaline etching are present, pore formation will initiate at these pits. Using this technique, a two-dimensional triangular lattice of pores was generated with a lattice constant of 2.3  $\mu\text{m}$ , a pore diameter of 1.7  $\mu\text{m}$ , and a depth of 75  $\mu\text{m}$ . Then, a micromachining technique, developed for structuring the porous layer, was used to produce small bars of porous material with steep side walls through which the transmission could be measured. The details of the technique are described elsewhere.<sup>24</sup> Briefly, photolithographically defined parts of the porous layer are etched away by an anisotropic plasma etching process yielding vertical walls. Afterwards, the diameter of the pores was widened to 2.13  $\mu\text{m}$  by subsequent thermal oxidation of the pore walls and etching of the oxide in hydrofluoric acid. Figure 1(a) shows an SEM micrograph of the patterned and micromachined layer. The bars of the porous layer remaining on the silicon substrate are 200  $\mu\text{m}$  wide (in *x* or *y* directions) and 75  $\mu\text{m}$  deep (in the *z* direction). Figure 1(b) shows a tenfold magnification of the inset in Fig. 1(a). The edges of the bars were formed by micromechanically etching the porous layer. The resulting walls were steep and sufficiently smooth for coupling light from the ambient air into the photonic lattice. Figure 1(c) shows another tenfold magnification of the inset of Fig. 1(b). In order to reveal the microstructure, one side of the bar was polished to show a plane 45° inclined to the sample surface. The lattice constant of the macropore array is 2.3  $\mu\text{m}$ , the pore diameter 2.13  $\mu\text{m}$ , and the thinnest parts of the pore walls 170 nm. This yields a porosity of the sample of 78%.

In order to theoretically calculate the band structure of this photonic lattice, the plane wave method as outlined in Refs. 18 and 25 was employed, where both the electromagnetic field and the periodic dielectric structure are expanded

<sup>a)</sup>Electronic mail: hermann.wendt@zfe.siemens.de

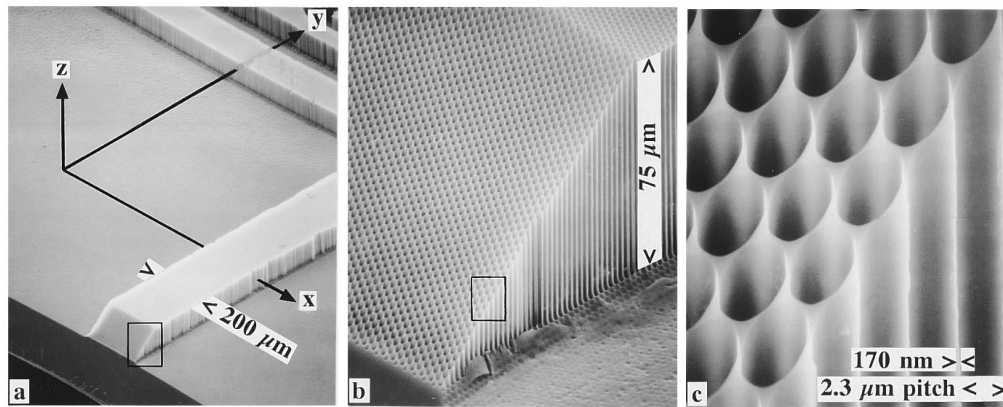


FIG. 1. Scanning electron micrographs of a patterned and micromachined layer of macroporous silicon forming a two-dimensional triangular lattice. (a) The  $200 \mu\text{m}$  wide and  $75 \mu\text{m}$  high bars of porous silicon are produced by micromechanically etching the porous layer. (b) A tenfold magnification of the inset in (a) is shown. The edges of the bars were formed by micromechanically etching the layer. (c) A tenfold magnification of the inset in (b) is shown. In order to reveal the microstructure, one side of the bar was polished to show a plane  $45^\circ$  inclined to the sample surface. The lattice constant of the macropore array is  $2.3 \mu\text{m}$ , the pore diameter  $2.13 \mu\text{m}$ , and the thinnest parts of the pore walls  $170 \text{ nm}$ .

in a Fourier series. For propagation of radiation in the plane of periodicity ( $x$ - $y$  plane), the two possible polarizations decouple, leading to two scalar problems. They are referred to as the  $E$  ( $E$ -field parallel to the pore axis) and  $H$  ( $H$ -field parallel to the pore axis) polarizations, respectively. For the calculations, a total number of 717 plane waves was used to ensure converged results. The Brillouin zone of the triangular lattice is shown in the inset of Fig. 2(a). The results for a lattice constant of  $2.3 \mu\text{m}$ , a hole diameter of  $2.13 \mu\text{m}$ , and a dielectric constant  $\epsilon$  of Si of 11.7

are presented in the center part of Figs. 2(a) and 2(b) for both  $H$  and  $E$  polarizations, respectively. A large photonic band gap exists between  $1501$  and  $2257 \text{ cm}^{-1}$  for the  $H$  polarization and a smaller one between  $1884$  and  $2182 \text{ cm}^{-1}$  for the  $E$  polarization, which determines the 15% wide, polarization-independent two-dimensional gap centered at  $2033 \text{ cm}^{-1}$  ( $4.9 \mu\text{m}$ ).

The transmission was measured along the  $\Gamma$ - $M$  or along the  $\Gamma$ - $K$  direction of the photonic lattice [see inset of Fig. 2(a)], where  $\Gamma$ - $M$  and  $\Gamma$ - $K$  correspond to the  $x$  and  $y$  directions in Fig. 1(a). The silicon substrate was broken in strips of several millimeter thickness along the  $x$  or  $y$  direction with a porous silicon bar at the center. The edges of the silicon substrate were covered with silver paint in order to avoid transmission through the substrate. Then, several pieces with the same lattice orientation were stacked in the  $z$  direction. Transmission was measured between  $500$  and  $3500 \text{ cm}^{-1}$  ( $2.9$ - $20 \mu\text{m}$ ) with a resolution of  $4 \text{ cm}^{-1}$ , using a standard FT-IR spectrometer (Nicolet 740), composed of a global source and a DTGS detector. A Perkin-Elmer gold wire grid polarizer was used for polarization-resolved measurements. The spectrum of the source was used as reference for normalization of the transmission spectra. However, as the transmitting area was not determined, no absolute values of the transmittance could be obtained in this way.

The transmission spectra of the sample are shown in Fig. 2(a) for  $H$  and in Fig. 2(b) for  $E$  polarization for both the wavevector  $k$  parallel to the  $\Gamma$ - $M$  direction (left side of Fig. 2) and  $k$  parallel to the  $\Gamma$ - $K$  direction (right side). For the  $H$  polarization [Fig. 2(a)], a sharp drop of the transmission is observed in the gap regions by more than two orders of magnitude for both the  $\Gamma$ - $M$  and the  $\Gamma$ - $K$  direction, in excellent agreement with the calculated band structure. For the  $E$  polarization [Fig. 2(b)], the overall transmission is smaller than for the  $H$  polarization by nearly one order of magnitude. Transmitting regions for  $E$ -polarized radiation are clearly observed in the spectral parts corresponding to the first, second, and fifth band for the  $\Gamma$ - $M$  direction, and to the first band for the  $\Gamma$ - $K$  direction, whereas the excitation of the other band seems to be either missing or inefficient.

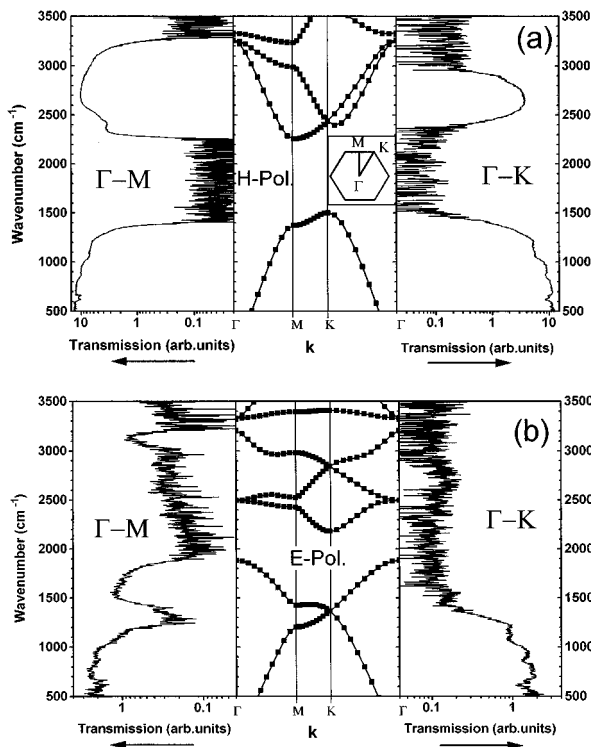


FIG. 2. In the center part, the calculated photonic band structure of the two-dimensional triangular lattice shown in Fig. 1 is plotted, the inset showing the first Brillouin zone. On the left-(right)-hand side, the transmission spectra of the sample for the  $\Gamma$ - $M$  ( $\Gamma$ - $K$ ) direction are shown between  $500$  and  $3500 \text{ cm}^{-1}$  (a) for  $H$ -polarized and (b) for  $E$ -polarized radiation. Note that the transmission is plotted on a logarithmic scale.

Concerning the values of the transmittance, it should drop to zero within the band gaps. However, the measured attenuation in the gap regions was limited both by the sensitivity of the detector and leakage paths around the photonic lattice, resulting in the observed noise in the forbidden regions. For the *H* polarization, the transmitted intensity in the allowed region is in the same order of magnitude for the first and second band. This is evidence that scattering within the porous sample and especially at the sample interface is only very weak, because otherwise one would expect increased scattering and hence decreased transmittance for decreasing wavelengths. The straight and smooth sample interface produced by the micromachining technique apparently allows efficient coupling of the radiation from the air into the photonic lattice. The relative intensity of the transmitting regions shows that *E*-polarized bands can either not be excited as efficiently as *H*-polarized bands or are more susceptible to scattering. The missing or inefficient excitation of some bands has been ascribed to symmetry constraints existing for the excitation by plane waves.<sup>8,9</sup>

The applied micromachining technique has proved to be a valuable tool for structuring the porous layer on a 10  $\mu\text{m}$  scale. This possibility may be essential if one wants to investigate single defect structures, as the radiation has to be coupled in and out of the defect through the photonic lattice and the macropores are etched in a macroscopic array.

In conclusion, we have succeeded in fabricating a two-dimensional photonic band gap structure in macroporous silicon with a complete band gap in the infrared region centered at 4.9  $\mu\text{m}$ . For the first time, the photonic lattice was micro-mechanically structured in order to produce 200  $\mu\text{m}$  wide free-standing bars of macroporous silicon with smooth interfaces through which the transmission was measured. The transmission spectra agreed very well with theoretical calculations and showed the high quality obtained by the fabrication technique. As pore growth can be observed for pore diameters as small as 100 nm, the high energy limit of macroporous silicon as photonic band gap material seems to be set by the (electronic) band gap of silicon at 1.1 eV. Thus, macroporous silicon appears to be one of the most promising photonic band gap materials in the infrared region.

We are grateful to Professor R. Helbig, F. Engelbrecht, and M. Neidel from the University Erlangen-Nürnberg for the use of and help with the FT-IR spectrometer. Theoretical calculations were partially supported by SFB 195 "Lokalisierung von Elektronen in makroskopischen und mikroskopischen Systemen." Siemens AG assisted in meeting the publication costs.

- <sup>1</sup>E. Yablonovitch, Phys. Rev. Lett. **58**, 2059 (1987).
- <sup>2</sup>S. John, Phys. Rev. Lett. **58**, 2486 (1987).
- <sup>3</sup>D. R. Smith, S. Schultz, N. Kroll, M. Sigalas, K. M. Ho, and C. M. Soukoulis, Appl. Phys. Lett. **65**, 645 (1994).
- <sup>4</sup>For a review, see the articles in *Photonic Bandgaps and Localization*, edited by C. M. Soukoulis, NATO ASI Series B (Plenum, New York, 1993), Vol. 308.
- <sup>5</sup>See also the special issues of J. Opt. Soc. Am. B **10**, No. 2 (1993) and J. Mod. Optics **41**, 171 (1994).
- <sup>6</sup>R. D. Meade, A. Devenyi, J. D. Joannopoulos, O. L. Alerhand, D. A. Smith, and K. Kash, J. Appl. Phys. **75**, 4753 (1994).
- <sup>7</sup>S. L. McCall, P. M. Platzman, R. Dalichaouch, D. Smith, and S. Schultz, Phys. Rev. Lett. **67**, 2017 (1991).
- <sup>8</sup>W. M. Robertson, G. Arjavalingam, R. D. Meade, K. D. Brommer, A. M. Rappe, and J. D. Joannopoulos, Phys. Rev. Lett. **68**, 2024 (1992).
- <sup>9</sup>R. D. Meade, K. D. Brommer, A. M. Rappe, and J. D. Joannopoulos, Appl. Phys. Lett. **61**, 495 (1992).
- <sup>10</sup>E. Yablonovitch, T. J. Gmitter, and K. M. Leung, Phys. Rev. Lett. **67**, 2295 (1991).
- <sup>11</sup>E. Yablonovitch, T. J. Gmitter, R. D. Meade, A. M. Rappe, K. D. Brommer, and J. D. Joannopoulos, Phys. Rev. Lett. **67**, 3380 (1991).
- <sup>12</sup>K. M. Ho, C. T. Chan, C. M. Soukoulis, R. Biswas, and M. Sigalas, Solid State Commun. **89**, 413 (1994).
- <sup>13</sup>E. Özbay, E. Michel, G. Tuttle, R. Biswas, M. Sigalas, and K.-M. Ho, Appl. Phys. Lett. **64**, 2059 (1994).
- <sup>14</sup>K. M. Leung and Y. F. Liu, Phys. Rev. Lett. **65**, 2646 (1990).
- <sup>15</sup>Z. Zhang and S. Satpathy, Phys. Rev. Lett. **65**, 2650 (1990).
- <sup>16</sup>K. M. Ho, C. T. Chan, and C. M. Soukoulis, Phys. Rev. Lett. **65**, 3152 (1990).
- <sup>17</sup>J. B. Pendry and A. MacKinnon, Phys. Rev. Lett. **69**, 2772 (1992).
- <sup>18</sup>M. Plihal and A. A. Maradudin, Phys. Rev. B **44**, 8565 (1991).
- <sup>19</sup>J. R. Wendt, G. A. Vawter, P. L. Gourley, T. M. Brennan, and B. E. Hammons, J. Vac. Sci. Technol. B **11**, 2637 (1993).
- <sup>20</sup>J. M. Gerard, A. Izraël, J. Y. Marzin, R. Padjen, and F. R. Ladan, Solid State Electron. **37**, 1341 (1994).
- <sup>21</sup>K. Inoue, M. Wada, K. Sakoda, A. Yamanaka, M. Hayashi, and J. W. Haus, Jpn. J. Appl. Phys. **33**, L1463 (1994).
- <sup>22</sup>V. Lehmann, J. Electrochem. Soc. **140**, 2836 (1993).
- <sup>23</sup>U. Grüning, V. Lehmann, and C. M. Engelhardt, Appl. Phys. Lett. **66**, 3254 (1995).
- <sup>24</sup>S. Ottow, V. Lehmann, and H. Föll, J. Electrochem. Soc. **143**, 385 (1996).
- <sup>25</sup>A. A. Maradudin and A. C. McGurn, in Ref. 4, p. 247.